Global and Regional Effects of Type 2 Diabetes on Brain Tissue Volumes and Cerebral Vasoreactivity

Published in final edited form as:
Diabetes Care. 2007 May ; 30(5): 1193–1199.

Global and Regional Effects of Type 2 Diabetes on Brain Tissue Volumes and Cerebral Vasoreactivity

David Last, PHD[1], **Cedric de Bazelaire, MD**[2], **David C. Alsop, PHD**[2], **Kun Hu, PHD**[1], **Amir M. Abduljalil, PHD**[3], **Jerry Cavallerano, OD, PHD**[4], **Robert P. Marquis, BS**[2], and **Vera Novak, MD, PHD**[1]

1 *Division of Gerontology, Beth Israel Deaconess Medical Center, Harvard Medical School, Boston, Massachusetts*

2 *Department of Radiology, Beth Israel Deaconess Medical Center, Harvard Medical School, Boston, Massachusetts*

3 *Department of Radiology, Ohio State University, Columbus, Ohio*

4 *Beetham Eye Institute, Joslin Diabetes Center, Boston, Massachusetts.*

Abstract

OBJECTIVE——The aim of this study was to evaluate the regional effects of type 2 diabetes and associated conditions on cerebral tissue volumes and cerebral blood flow (CBF) regulation.

RESEARCH DESIGN AND METHODS——CBF was examined in 26 diabetic (aged 61.6 ± 6.6 years) and 25 control (aged 60.4 ± 8.6 years) subjects using continuous arterial spin labeling (CASL) imaging during baseline, hyperventilation, and CO_2 rebreathing. Regional gray and white matter, cerebrospinal fluid (CSF), and white matter hyperintensity (WMH) volumes were measured on a T1-weighted inversion recovery fast-gradient echo and a fluid attenuation inversion recovery magnetic resonance imaging at 3 Tesla.

RESULTS——The diabetic group had smaller global white ($P = 0.006$) and gray ($P = 0.001$) matter and larger CSF (36.3%, $P < 0.0001$) volumes than the control group. Regional differences were observed for white matter (−13.1%, $P = 0.0008$) and CSF (36.3%, $P < 0.0001$) in the frontal region, for CSF (20.9%, $P = 0.0002$) in the temporal region, and for gray matter (−3.0%, $P = 0.04$) and CSF (17.6%, $P = 0.01$) in the parieto-occipital region. Baseline regional CBF ($P = 0.006$) and CO_2 reactivity ($P = 0.005$) were reduced in the diabetic group. Hypoperfusion in the frontal region was associated with gray matter atrophy ($P < 0.0001$). Higher A1C was associated with lower CBF ($P < 0.0001$) and greater CSF ($P = 0.002$) within the temporal region.

CONCLUSIONS——Type 2 diabetes is associated with cortical and subcortical atrophy involving several brain regions and with diminished regional cerebral perfusion and vasoreactivity. Uncontrolled diabetes may further contribute to hypoperfusion and atrophy. Diabetic metabolic disturbance and blood flow dysregulation that affects preferentially frontal and temporal regions may have implications for cognition and balance in elderly subjects with diabetes.

Diabetes is a prevalent condition associated with substantial morbidity attributed to vascular complications (1). Diabetes alters endothelial function (2) and permeability of the blood-brain barrier, thus affecting micro-circulation and regional metabolism (3). Studies in type 1 diabetes have shown that the fronto-temporal cortex and periventricular white matter (3) are more affected by diabetic metabolic disturbance. Single proton emission computed tomography

Address correspondence and reprint requests to Vera Novak, MD, PhD, Division of Gerontology, Beth Israel Deaconess Medical Center, 110 Francis St., Boston, MA 02215. E-mail: vnovak@bidmc.harvard.edu.

A table elsewhere in this issue shows conventional and Système International (SI) units and conversion factors for many substances.

(SPECT) studies suggest that chronic hyperglycemia alters cerebral blood flow (CBF) in the frontal, temporal, parietal, occipital, and cerebellar regions of interest (ROIs) (4,5). Vasoreactivity to acetazol-amide is not homogeneous, with a majority of hypoperfused and some hyperperfused ROIs (6). White matter hyperintensities (WMHs) on T2-weighted magnetic resonance imaging (MRI) (7) have been associated with arteriolosclerosis, arising as consequences of aging, diabetes, and other cardiovascular risk factors (8,9). Vascular and neurodegenerative changes in these structures have consequences for regional perfusion, cognitive impairment, and balance in elderly people with type 2 diabetes (10,11). We hypothesize that type 2 diabetes is associated with microvascular disease, manifesting as WMHs and CBF dysregulation and neuronal loss affecting preferentially fronto-temporal regions. We aimed to determine the effects of type 2 diabetes on regional brain volumes and vasoreactivity using anatomical imaging and continuous arterial spin labeling (CASL) blood flow MRI at 3 Tesla (12,13).

RESEARCH DESIGN AND METHODS—

Studies were conducted at the Syncope and Falls in the Elderly Laboratory and at the MRI Center at the Beth Israel Deaconess Medical Center using a GE 3-Tesla VHI scanner with a quadrature head coil. All subjects were recruited consecutively and provided informed consent approved by the institutional review board. The study control groups consisted of 25 healthy subjects who were normotensive and not being treated for any systemic disease and 26 subjects with type 2 diabetes (Table 1). All subjects were screened with a medical history and physical and laboratory examinations. Diabetic subjects were treated with insulin (9), oral glucose control agents (sulfonylureas and second-generation agents (7), meglitinides (1), thiazolidinediones (4), and biguanides (8) and their combinations (13) or with diet (4), as well as for hypertension when clinically diagnosed (8). Diabetic retinopathy was diagnosed with video-digital retinal imaging in 10 diabetic patients in the Joslin Vision Network (14). Statins were used in four control and eight diabetic subjects. Urinary albumin, creatinine, and their ratio were not different between the groups. Diabetic subjects reported symptoms of dizziness (4) and syncope (2), orthostatic hypotension (2), numbness (8), and peripheral neuropathy (3). Subjects with a history of stroke, myocar-dial infarction, congestive heart failure, and other clinically important cardiac diseases, arrhythmias, significant nephropathy, kidney or liver transplant, renal failure, carotid artery stenosis, and neurological or other systemic disorders were excluded. Subjects with MRI-incompatible metal implants, pacemakers, arterial stents, and claustrophobia also were excluded.

MRI

Anatomical imaging protocol included T1-weighted inversion recovery fast-gradient echo (IR-FGE) ($T_I/T_E/T_R$ = 600/3.3/8.1 ms, 24 × 19–cm field of view, 256 × 192 matrix size, and 3-mm slice thickness [no skip]) and fluid-attenuated inversion recovery (FLAIR) ($T_I/T_E/T_R$ = 2,250/161/11,000 ms, 24 × 24–cm field of view, 256 × 160 matrix size, and 5-mm slice thickness [1.5 mm skip]). CASL MRI was used for blood flow measurements (12,13). An echo planar imaging sequence was applied with T_E = 31 ms, 24 × 24 cm field of view, 64 × 64 matrix size, and 5-mm slice thickness (5 mm skip) for eight slices starting at the level of ventricles. Tagged and control images were collected over 5-min periods of normal breathing, CO_2 rebreathing of 95% air and 5% CO_2, and hyperventilation. Images were obtained every 8 s and averaged for each condition. End-tidal CO_2 was continuously monitored and averaged over 15-s intervals for all conditions. A CBF map was reconstructed for each condition, as previously described (ml · 100 g^{-1} · min^{-1}) (12,13), and corrected for the effect of hematocrit on T1 (15).

Image analysis

All image data were processed on a Linux workstation, using tools developed in the IDL programming environment (Research Systems, Boulder, CO). Figure 1A presents an example of IR-FGE (I1) and FLAIR (F1) images and a T2 reference image used for CBF map reconstruction (C1). First, a three-dimensional ROI corresponding to the parenchymal brain was extracted using the "brain extraction tools" algorithm (16) on the IR-FGE and the FLAIR images and by simple thresholding of the T2 reference image for the CBF maps. Each ROI was divided into eight regions. On each axial slice, an ellipse was fitted to the edge of the brain using a nonlinear least-squares method. The medial axis of the smallest rectangle to enclose the ellipse was computed with the ellipse parameters. This first step allowed the delineation of six regions on all axial slices: the frontal, temporal, and parieto-occipital for each hemisphere were separated using the ellipse major axis (Fig. 1A, I2). Supraventricular slices were analyzed as one region and named the cortical region. This region definition was proposed by Dahl et al. (17) for quantification of regional perfusion using SPECT. It was applied to outline the same eight regions on all ROIs without any registration step, as illustrated on Fig. 1A (I2, F2, and C2). Regions outline major intracranial vascular territories and the frontal, temporal, and parieto-occipital lobes. A relative limitation is that these regions do not follow the precise anatomical boundaries and therefore may include small areas with different functions. Accordingly, our goal was to quantify the global differences in distribution of CBF and vascular reactivity to CO_2 rather than responses to local activation.

The expectation-maximization algorithm was used to assess gray matter, white matter, and cerebrospinal fluid (CSF) volumes by segmenting the IR-FGE ROI into three classes (Fig. 1A, I3). The expectation-maximization method (18,19) estimates iteratively the parameters of a model of the image histogram (three Gaussian distributions) by maximizing the likelihood of the distribution. On the FLAIR ROI, WMH seeds were identified using thresholding of hyperintense pixels. Borders of WMHs were then detected using a simple region-growing method applied on WMH seeds, yielding a connected WMH cluster for each seed (Fig. 1A, F3). The volumes of the whole brain and of the eight regions were computed on the IR-FGE images. Gray matter, white matter, and CSF volumes were normalized for the volume of each region on the segmented IR-FGE images (Fig. 1A, I4). WMH volume was normalized for the volume of each region on the segmented FLAIR images (Fig. 1A, F4). Each CBF map (Fig. 1A, C3) was averaged within each region for each breathing exercise (Fig. 1A, C4). CO_2 reactivity was computed in each region as the slope of the linear fit between end-tidal CO_2 and CBF values for each condition. Relative reactivity also was calculated as a percentage change in CBF and CO_2 between hyper-ventilation and rebreathing.

Statistical analysis

Descriptive statistics were used to summarize all variables. Demographic and laboratory variables were compared between groups using one-way ANOVA and Fisher's exact test. The volumes (whole brain and in regions), the normalized gray and white matter, CSF, and WMH regional volumes were compared between the control and diabetic groups using the least-square models with adjustments for age, sex, regions, and hemisphere side. CBF and CO_2 reactivity comparisons between the groups and conditions (baseline, CO_2 rebreathing, and hyper-ventilation) also include hematocrit and BMI as covariants. Stepwise multiple regression and least-square models also were used to test the effects of A1C, triglycerides, systolic blood pressure, and BMI as continuous variables in the model. The effects of diabetic retinopathy, hypertension, and neuropathy were included as nominal variables and evaluated using the same approach.

RESULTS

Demographic and laboratory measures

Table 1 compares the demographic characteristics and intracranial brain volume of the control and the diabetic groups. Age, sex, and race did not differ between the groups. Diabetic subjects had higher BMI ($P = 0.01$), A1C ($P < 0.0001$), blood glucose ($P = 0.002$), systolic blood pressure ($P = 0.04$), and cholesterol ($P = 0.007$) but lower hematocrit ($P = 0.02$).

Regional intracranial volumes

The regional volumes were similar between the groups, except for the cortical region, which was smaller in the diabetic group ($P = 0.007$). Figure 1B–E shows normalized volumes of white and gray matter, CSF, and WMHs in the frontal, temporal, parieto-occipital, and cortical regions for both groups. Over all regions, the diabetic group had smaller white ($P = 0.006$, Fig. 1B) and gray ($P = 0.001$, Fig. 1C) matter volume but larger CSF volume ($P < 0.0001$, Fig. 1D) than the control group. This difference also was observed for white matter (−13.1%, $P = 0.0008$) and CSF (36.3%, $P < 0.0001$) in the frontal region, for CSF (20.9%, $P = 0.0002$) in the temporal region, and for gray matter (−3.0%, $P = 0.04$) and CSF (17.6%, $P = 0.01$) in the parieto-occipital region. In the control and diabetic groups, normalized WMH volume differed between regions ($P < 0.0001$). WMH volume was greater in the temporal ($P < 0.0001$) and frontal regions and smaller in the parieto-occipital ($P = 0.03$) and cortical ($P < 0.0001$) regions (Fig. 1E). WMH volume increased with age ($P < 0.0001$, $r = 0.49$) and was higher in the left hemisphere ($P = 0.004$). Presence of diabetic retinopathy was associated with greater CSF within the temporal region ($r = 0.58$, $P = 0.0003$). Diabetic subjects with hypertension had increased CSF volume ($P < 0.0001$) and decreased gray matter volume ($P = 0.008$) and greater CSF volume in frontal ($P < 0.0001$) and temporal ($P = 0.03$) regions and greater gray matter volume in the frontal region ($P = 0.05$) compared with normotensive diabetic subjects. In the diabetic group, A1C was associated with more atrophy (CSF: $r = 0.72$, $P = 0.002$) within the temporal region.

CBF and CO_2 reactivity

Figure 2 shows T2 reference images and the corresponding CBF maps for baseline, CO_2 rebreathing, and hyperventilation for a control subject (Fig. 2A–D) and a diabetic subject (Fig. 2E–H). CBF differed among test conditions ($P < 0.0001$) in both groups. During baseline rest, the regional CBF was higher in the parieto-occipital ($P < 0.0001$) and lower in the frontal ($P = 0.0005$) and temporal ($P = 0.02$) regions in both groups (Fig. 2I). Over all regions, CBF was lower in the diabetic group than in the control group during normal breathing ($P = 0.006$) and CO_2 rebreathing ($P = 0.001$) but was similar during hyperventilation. Figure 2J shows group CO_2 reactivity values that were lower in the diabetic group than in the control group ($P = 0.005$) over all regions. Relative CO_2 reactivity values also were lower in the diabetic group ($P = 0.02$). For all conditions, CO_2 values did not differ between groups (control: 36.1 ± 5.3 mmHg; diabetes: 37.0 ± 4.3 mmHg during baseline rest).

CBF during baseline was positively associated with regional gray matter volume ($r = 0.77$, $P < 0.0001$), reflecting CBF decline in frontal regions ($P < 0.0001$) and increases in the parieto-occipital regions ($P = 0.003$) in both groups. In the frontal region, steeper slope of regression (4.99 vs. 2.7) indicated greater CBF decline in the diabetic group. WMHs were associated with reduced CO_2 reactivity ($r = −0.54$, $P = 0.0004$) in the control group and contributed to regional differences in vasoreactivity ($P = 0.001$) in the diabetic group. In the diabetic group, retinopathy and hypertension were associated with lower CBF during hypercapnia ($r = −0.61$, $P = 0.0008$ and $r = −0.61$, $P = 0.002$, respectively) and hypocapnia ($r = −0.77$, $P = 0.05$ and $r = −0.80$ $P = 0.003$, respectively). These associations were observed within the temporal region, during hypercapnia for retinopathy ($P = 0.03$), and during hypercapnia ($P = 0.02$) and hypocapnia ($P = 0.04$) for hypertension. Higher BMI was associated with lower CBF in both groups ($r =$

−0.66, $P < 0.01$). In the diabetic group, higher A1C was associated with lower CBF ($r = -0.78$, $P < 0.0001$) and lower CO_2 reactivity ($r = -0.45$, $P = 0.009$). Higher baseline systolic blood pressure was associated with lower CBF ($r = -0.41$, $P < 0.002$). Triglycerides had no significant effect on CBF. Retinopathy was associated with lower CO_2 reactivity ($r = -0.47$, $P = 0.03$).

CONCLUSIONS—

This study demonstrated that cortical and subcortical atrophy in type 2 diabetes is associated with diminished regional cerebral perfusion and vasoreactivity. Brain atrophy, as indicated by CSF volume, was prominent in the frontal and temporal regions. Hypoperfusion during baseline rest and diminished CBF response to hypercapnia affected all regions. A1C levels and diabetic retinopathy were further associated with CBF reduction, altered vasoreactivity, and atrophy that was most prominent in the temporal region. This study focused on neuroasymptomatic subjects; therefore, those with significant late complications of diabetes and history of cerebrovascular accidents that may further affect CBF were excluded. Cerebromicrovascular disease and endothelial dysfunction affect multiple brain regions and vascular territories and are associated with CBF dysregulation beyond the brain atrophy.

Hyperglycemia is a unifying mechanism for diabetic tissue damage in the brain, as glucose utilization requires transport through the blood-brain barrier and metabolism to provide energy supply (20). Altered glucose transporter regulation results in intracellular hyperglycemia in endothelial cells and neurons (21,22). Signaling of oxidative stress (23,24) in mitochondria and the endoplasmic reticulum leads to activation of four major cell-damaging pathways. Superoxide also triggers an inflammatory response through the release of proinflammatory cytokines (i.e., tumor necrosis factor α, endothelin-1, and interleukins) and decreased synthesis of nitric oxide. These cascades activate proapoptotic pathways and ultimately cause neuronal cell damage and death. The finding that *N*-acetyl aspartate (an indicator of functional neuronal mass) was reduced in hypertensive diabetic patients in the areas affected by WMHs supports the notion that neuronal loss in frontal and temporal associative areas may contribute to functional decline in type 2 diabetes (25). In our study, WMHs were associated with regional differences in white matter volume, vasore-activity, and higher A1C. These results support the theory that hyperglycemia in association with other mechanisms (i.e., those related to oxidative stress) may contribute to neurodegeneration in diabetic brain in addition to endothelial dysfunction.

Our results demonstrating reduced CBF in type 2 diabetes are consistent with CBF abnormalities reported in earlier studies. Semiquantitative assessments of regional CBF using SPECT detected the lower ratio between regions with normal CBF versus areas of reduced CBF in type 1 diabetic subjects (4,5). The ratio was inversely correlated with systolic blood pressure, total cholesterol, and the atherogenic index, and it was positively correlated with HDL and cholesterol. These observations suggest that the age-related CBF reduction may be accelerated by a combination of hyperglycemia plus other risk factors for arteriosclerosis (26,27). The regional differences in cerebral metabolic capacity may explain increased sensitivity to hyperglycemia in the cerebral cortex (28). Previous studies described reduced or normal CO_2 reactivity in diabetes (32,33). This study applying CASL for evaluation of CBF and CO_2 vasoreactivity demonstrated that CASL is a reliable tool for assessment of flow reserve in an elderly diabetic population.

There may be some limitations to this approach. Because of the short decay time of the CASL label (~1 s), CBF measurements might be affected for longer arterial transit time at low flow as during hypocapnia. It is important to mention that CBF measurements that reflect mainly flow in the gray matter were normalized for the volume of the ROI on which they were computed and also were adjusted for any variability associated with age, sex, hematocrit, and

BMI to adjust for the effects of tissue loss and possible effects of other variables and risk factors. Therefore, the observed CBF changes are unlikely to be affected by partial volume effects attributed to an increased CSF. Our region selection approach allowed comparisons among different brain areas' anatomical and CBF images. As the method did not require any registration step, the definition of identical regions on all ROIs was performed regardless of the differences in matrix and voxel size between IR-FGE, FLAIR, and CASL images. We validated our automated method of WMH quantification, and we found excellent correlations between WMH volume and clinical rating scale (35).

The segmentation method of the IRFGE image allows accurate classification of noisy pixels and, thus, reliable measurements of CSF volume that have been validated using the phantom model (36). Regional intensity variation caused by an inhomogeneous radiofrequency coil and low signal-to-noise ratio, however, may reduce the accuracy of the brain tissue classification. The electron microscope–based segmentation method was selected because it can estimate the intensity of inhomogenities. In addition, the voxel classification is influenced primarily by the neighboring voxels, reducing the difficulties encountered in noisy regions of the images (37). The relatively thick 5-mm slices and 1.5-mm gaps in the FLAIR images may be a contributor to errors in the measurement of the WMHs. To estimate this uncertainty, a high-resolution model of the WMHs was created with the same parameters. Then, an axial offset to the slices' position was introduced, and the volume was calculated as a function of this offset. It is estimated that a ±6% uncertainty in the measured WMH volume is introduced by the selected geometry of the FLAIR images (36).

Microvascular and macrovascular disease and neurodegeneration in type 2 diabetes has been associated with accelerated cognitive impairment and dementia in elderly subjects (38). Diagnosis of diabetes doubled the risk for both hippocampal atrophy and lacunar infarcts in a population-based study. Diabetic patients with the longest disease duration, those taking insulin, and those with complications had more severe pathologic brain abnormalities (39). Diabetes also is associated with cortical and subcortical atrophy, WMHs, and impaired cognitive performance (attention and executive function, information processing speed, and memory) (11). Elevated body mass and systemic pressure may further affect cerebral perfusion and contribute to cognitive decline in older people (40).

Some limitations to our approach may arise from the fact that selected regions reflect more vascular territories rather than anatomical regions and that slice thickness on FLAIR images may affect WMH volume estimates. The study was done on an outpatient basis, and laboratory values may include nonfasting samples. This study addressed an important question about the effects of type 2 diabetes on regional CBF distribution and vasomotor reserve in older adults and provided evidence for reduced perfusion beyond gray and white matter atrophy. Higher levels of A1C were associated with lower CBF and greater CSF volume in the temporal region. Reduced resting blood flow may reflect combined effects of microvascular disease and metabolic tissue damage affecting preferentially frontal and temporal regions. These findings are clinically relevant for functional outcomes, such as cognition and balance of elderly people with diabetes. Further study of the mechanisms prospectively relating hypoperfusion to neurodegeneration and functional outcomes in type 2 diabetes is merited.

Acknowledgments—

This study was supported by an American Diabetes Association Grant (1-03-CR-23 and 1-06-CR-25); the National Institutes of Health (NIH), National Institute of Neurological Disorders and Stroke (1R01-NS045745-01A21 [to V.N.]); an NIH Older American Independence Center Grant (2P60 AG08812); an NIH program project (AG004390); and a General Clinical Research Center Grant (MO1-RR01032).

Abbreviations

CASL, continuous arterial spin labeling; CBF, cerebral blood flow; CSF, cerebrospinal fluid; FLAIR, fluid-attenuated inversion recovery; IR-FGE, inversion recovery fast-gradient echo; MRI, magnetic resonance imaging; ROI, region of interest; SPECT, single proton emission computed tomography; WMH, white matter hyperintensity.

References

1. U.S. Department of Health and Human Services, Centers for Disease Control and Prevention. National Diabetes Fact Sheet: General Information and National Estimates on Diabetes in the United States, 2003. Revised ed.. Centers for Disease Control and Prevention; Atlanta, GA: 2004.
2. Trauernicht AK, Sun H, Patel KP, Mayhan WG. Enalapril prevents impaired nitric oxide synthase-dependent dilatation of cerebral arterioles in diabetic rats. Stroke 2003;34:2698–2703. [PubMed: 14563973]
3. Makimattila S, Malmberg-Ceder K, Hakkinen AM, Vuori K, Salonen O, Summanen P, Yki-Jarvinen H, Kaste M, Heikkinen S, Lundbom N, Roine RO. Brain metabolic alterations in patients with type 1 diabetes-hyperglycemia-induced injury. J Cereb Blood Flow Metab 2004;24:1393–1399. [PubMed: 15625413]
4. Vazquez LA, Amado JA, Garcia-Unzueta MT, Quirce R, Jimenez-Bonilla JF, Pazos F, Pesquera C, Carril JM. Decreased plasma endothelin-1 levels in asymptomatic type I diabetic patients with regional cerebral hypoperfusion assessed by Spect. J Diabetes Complications 1999;13:325–331. [PubMed: 10765011]
5. Jimenez-Bonilla JF, Carril JM, Quirce R, Gomez-Barquin R, Amado JA, Gutierrez-Mendiguchia C. Assessment of cerebral blood flow in diabetic patients with no clinical history of neurological disease. Nucl Med Commun 1996;17:790–794. [PubMed: 8895906]
6. Quirce R, Carril JM, Jimenez-Bonilla JF, Amado JA, Gutierrez-Mendiguchia C, Banzo I, Blanco I, Uriarte I, Montero A. Semi-quantitative assessment of cerebral blood flow with 99mTc-HMPAO SPET in type I diabetic patients with no clinical history of cerebrovascular disease. Eur J Nucl Med 1997;24:1507–1513. [PubMed: 9391186]
7. van Swieten JC, van den Hout JH, van Ketel BA, Hijdra A, van Gijn J. Periventricular lesions in the white matter on magnetic resonance imaging in the elderly: a morphometric correlation with arteriolosclerosis and dilated perivascular spaces. Brain 1991;114:761–774. [PubMed: 2043948]
8. deGroot JC, de Leeuw FE, Ouderk M, Hofman A, Jolles J, Breteler MM. Cerebral white matter lesions and subjective cognitive dysfunction: the Rotterdam Scan Study. Neurology 2001;56:1539–1541. [PubMed: 11402112]
9. Wahlund LO, Barkhof F, Fazekas F, Bronge L, Augustin M, Sjogren M, Wallin A, Ader H, Leys D, Pantoni L, Pasquier F, Erkinjuntti T, Scheltens P. A new rating scale for age-related white matter changes applicable to MRI and CT. Stroke 2001;32:1318–1322. [PubMed: 11387493]
10. Kannel WB, Kannel C, Paffenbarger RSJ, Cupples LA. Heart rate and cardiovascular mortality: the Framingham Study. Am Heart J 1987;113:1494.
11. Manschot SM, Brands AM, vander Grond J, Kessels RP, Algra A, Kappelle LJ, Biessels GJ. Brain magnetic resonance imaging correlates of impaired cognition in patients with type 2 diabetes. Diabetes 2006;55:1106–1113. [PubMed: 16567535]
12. Detre JA, Alsop DC, Vives LR, Maccotta L, Teener JW, Raps EC. Noninvasive MRI evaluation of cerebral blood flow in cerebrovascular disease. Neurology 1998;50:633–641. [PubMed: 9521248]
13. Alsop DC, Detre JA. Multisection cerebral blood flow MR imaging with continuous arterial spin labeling. Radiology 1998;208:410–416. [PubMed: 9680569]
14. Aiello LM, Cavallerano JD, Cavallerano AA, Bursell SE. The Joslin Vision Network (JVN) Innovative Telemedicine Care for Diabetes. Ophthalmol Clin North Am 2000;13:213–224.
15. Lu H, Clingman C, Golay X, van Zijl PCM. Determining the longitudinal relaxation time (T1) of blood at 3 Tesla. Magn Reson Med 2004;52:679–682. [PubMed: 15334591]
16. Smith SM. Fast robust automated brain extraction. Hum Brain Mapp 2002;17:143–155. [PubMed: 12391568]

17. Dahl A, Russel D, Nyberg-Hansen R, Rootwelt K. Effect of nitroglycerin on cerebral circulation measured by transcranial Doppler and SPECT. Stroke 1989;20:1733–1736. [PubMed: 2512693]
18. Wells WM, Kininis R, Grimson WEL, Jolesz F. Adaptive segmentation of MRI data. IEEE Trans Biomed Eng 1996;15:429–442.
19. Gering DT, Nabavi A, Kininis R, Hata N, O'Donnell LJ, Grimson WEL, Jolesz FA, Black PM, Wells WM. An integrated visualization system for surgical planning and guidance using image fusion and an open MR. J Magn Reson Imaging 2001;13:967–975. [PubMed: 11382961]
20. McCall AL. Cerebral glucose metabolism in diabetes mellitus. Eur J Pharmacol 2004;490:147–158. [PubMed: 15094081]
21. Wilterdink JL, Feldmann E. Cerebral hemorrhage. Adv Neurol 1994;64:13–23. [PubMed: 8291461]
22. Brownlee M. The pathobiology of diabetic complications. Diabetes 2006;54:1615–1625. [PubMed: 15919781]
23. Yu T, Robotham JL, Yoon Y. Increased production of reactive oxygen species in hyperglycemic conditions requires dynamic change of mitochondrial morphology. Proc Natl Acad of Sci U S A 2006;21:2653–2658. [PubMed: 16477035]
24. Monnier L, Mas E, Ginet C, Michel F, Villon L, Cristol JP, Colette C. Activation of oxidative stress by acute glucose fluctuations compared with sustained chronic hyperglycemia in patients with type 2 diabetes. JAMA 2006;295:1681–1687. [PubMed: 16609090]
25. Kario K, Ishikawa J, Hoshide S, Matsui Y, Morinari M, Eguchi K, Ishikawa S, Shimada K. Diabetic brain damage in hypertension: role of renin-angiotensin system. Hypertension 2005;45:887–983. [PubMed: 15824198]
26. Wakisaka M, Nagamachi S, Inoue K, Morotomi Y, Nunoi K, Fujishima M. Reduced regional cerebral blood flow in aged noninsulin-dependent diabetic patients with no history of cerebrovascular disease: evaluation by N-isopropyl-123I-p-iodoamphetamine with single-photon emission computed tomography. J Diabetes Complications 1990;4:170–174.
27. Keymeulen B, Jacobs A, de Metx K, de Sadeleer C, Bossuyt A, Somers G. Regional cerebral hypoperfusion in long-term type 1 (insulin-dependent) diabetic patients: relation to hypoglycaemic event. Nucl Med Commun 1995;16:10–16. [PubMed: 7609929]
28. Cranston I, Marsden P, Matyka K, Evans M, Lomas J, Sonksen P, Maisey M, Amiel SA. Regional differences in cerebral blood flow and glucose utilization in diabetic man: the effect of insulin. J Cereb Blood Flow Metab 1998;18:130–140. [PubMed: 9469154]
29. Fulesdi B, Limburg M, Bereczki D, Kaplar M, Molnar C, Kappelmayer J, Neuwirth G, Csiba L. Cerebrovascular reactivity and reserve capacity in type II diabetes mellitus. J Diabetes Complications 1999;13:191–199. [PubMed: 10616858]
30. Kadoi Y, Saito S, Goto F, Fujita N. The effect of diabetes on the interrelationship between jugular venous oxygen saturation responsiveness to phenylephrine infusion and cerebrovascular carbon dioxide reactivity. Anesth Analg 2004;99:325–331. [PubMed: 15271699]
31. Griffith DN, Saimbi S, Lewis C, Tolfree S, Betteridge DJ. Abnormal cerebrovascular carbon dioxide reactivity in people with diabetes. Diabet Med 1987;4:217–220. [PubMed: 2956022]
32. Kadoi Y, Hinohara H, Kunimoto F, Saito S, Ide M, Hiraoka H, Kawahara F, Goto F. Diabetic patients have an impaired cerebral vasodilatory response to hypercapnia under propofol anesthesia. Stroke 2003;34:2399–2403. [PubMed: 12958324]
33. Dandona P, James IM, Newbury PA, Woollard ML, Beckett AG. Cerebral blood flow in diabetes mellitus: evidence of abnormal cerebrovascular reactivity. Br Med J 1978;29:325–326. [PubMed: 687900]
34. van Oers CA, Manschot SM, Van Huffelen AC, Kappelle LJ, Biessels GJ. Cerebrovascular reserve capacity is preserved in a population-based sample of patients with type 2 diabetes mellitus. Cerebrovasc Dis 2006;22:46–50. [PubMed: 16567937]
35. Novak V, Last D, Alsop DC, Abduljalil AM, Hu K, Lepicovsky L, Cavallerano J, Lipsitz LA. Cerebral blood flow velocity and periventricular white matter hyperintensities in type 2 diabetes. Diabetes Care 2006;29:1529–1534. [PubMed: 16801574]
36. Firbank MJ, Coulthard A, Harrison RM, Williams ED. Partial volume effects in MRI studies of multiple sclerosis. Magn Reson Imaging 1999;17:593–601. [PubMed: 10231186]

37. Kapur T, Grimson WEL, Kininis R, Wells WM. Enhanced spatial parameters for segmentation of magnetic resonance imaging. Lect Notes Comput Sc 1998;457:458.

38. Cukierman T, Gerstein HC, Williamson JD. Cognitive decline and dementia in diabetes: systematic overview of prospective observational studies. Diabetologia 2005;48:2460–2469. [PubMed: 16283246]

39. Korf ES, White LR, Scheltens P, Launer LJ. Brain aging in very old men with type 2 diabetes: the Honolulu-Asia Aging Study. Diabetes Care 2006;29:2268–2274. [PubMed: 17003305]

40. Cournot M, Marquie JC, Ansiau D, Martinaud C, Fonds H, Ferrieres J, Ruidavets JB. Relation between body mass index and cognitive function in healthy middle-aged men and women. Neurology 2006;76:1208–1214. [PubMed: 17030754]

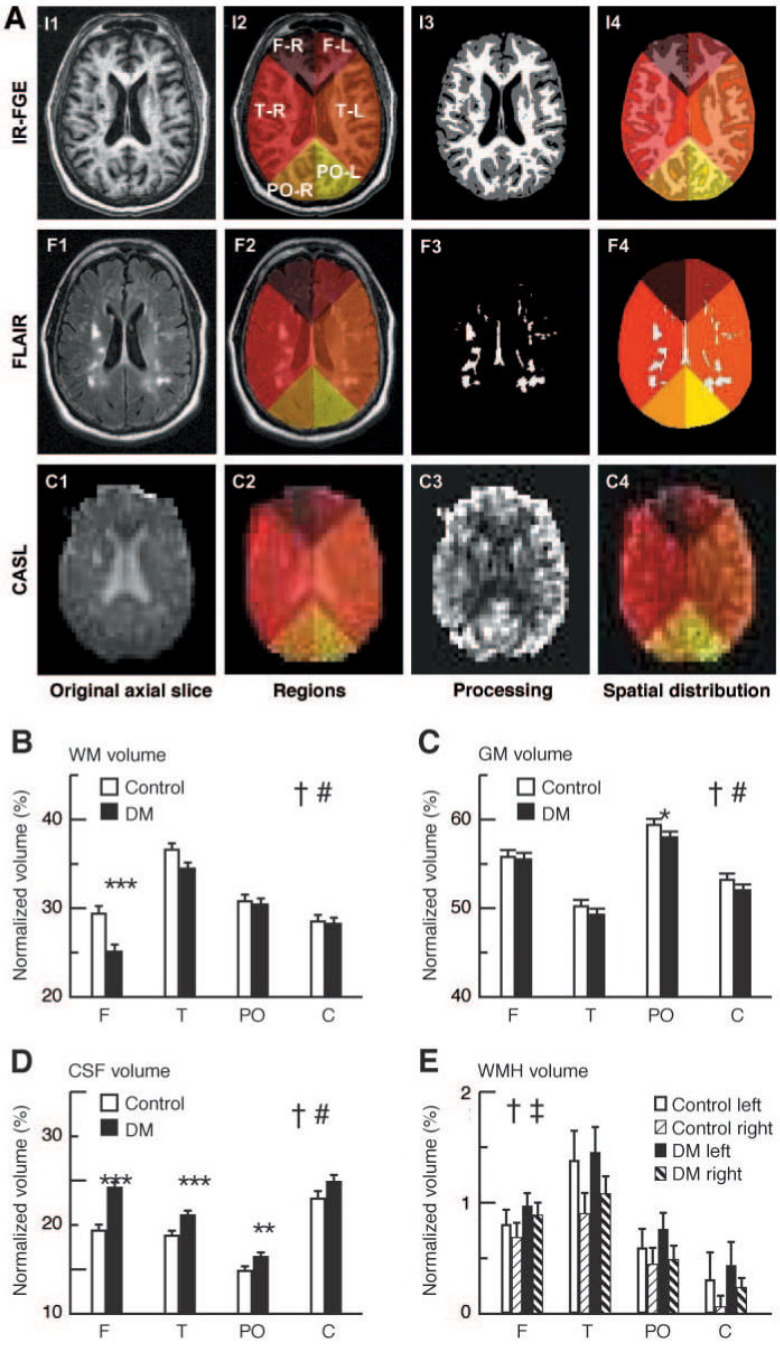

Figure 1.

A: Brain regions partitioning method. The first column on the left presents an original axial slice at the level of the ventricles for the IR-FGE (I1), the FLAIR image (F1), and for the CASL acquisition (T2 reference image, C1). The second column illustrates the six regions computed on the images showed on column 1: the left (L) and right (R) side of the frontal (F), parieto-occipital (PO), and temporal (T) regions (as indicated on I2). The last two columns illustrate the processing/reconstruction performed on the images shown in column 1 and the assessment of spatial distribution for the computed parameters. The regions were applied to the segmented IR-FGE image (I3) to assess the regional distribution of gray matter, white matter, and CSF volumes (I4) to the segmented FLAIR image (F3) to assess WMH volume distribution (F4).

After reconstruction of the (CBF) maps (an example CO_2 rebreathing map is shown on C3), CBF values were averaged over each region (C4), allowing CO_2 reactivity computation for each region. White matter (B), gray matter (C), CSF (D), and WMH (E) volumes in the frontal (F), temporal (T), parieto-occipital (PO), and cortical (C) regions for both groups, normalized for region volume in control and diabetic (DM) groups (means ± SE). †Between-region comparisons for both groups ($P < 0.0001$). ‡Between-hemisphere comparisons for both groups ($P = 0.004$). #Between-group comparisons over all regions ($P \leq 0.006$). ***Between-group comparisons within regions ($P \leq 0.0008$). *$P = 0.04$; **$P = 0.01$.

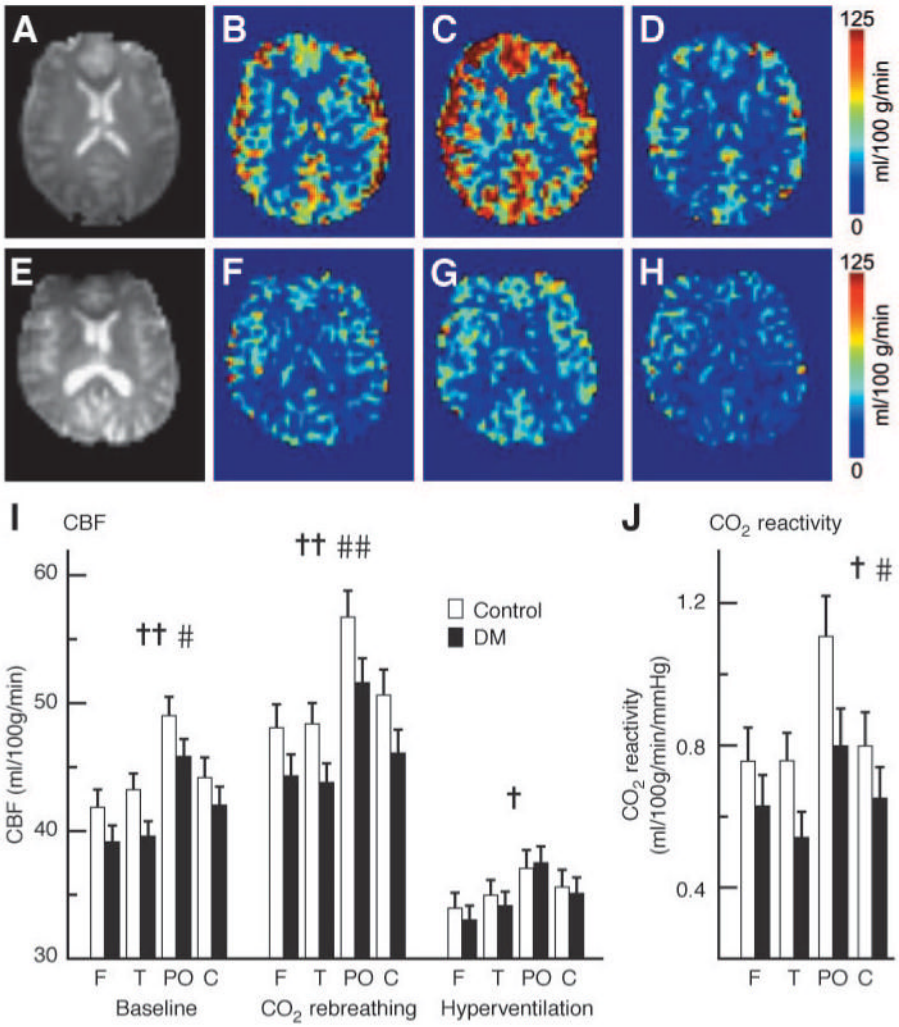

Figure 2.

CBF maps reconstructed from the CASL acquisition for a control subject (A–D) and a diabetic (DM) subject (E–G). A and E: An axial slice of a T2 reference image at the level of the ventricles used for the CBF map reconstruction. B and F: CBF maps at baseline. C and G: CO_2 rebreathing. D and H: Hyperventilation. The perfusion ranges from 0 to 125 ml · 100 g^{-1} · min^{-1} on all CBF maps. CBF during the first baseline, the CO_2 rebreathing, and hyperventilation periods (I) and the calculated CO_2 reactivity (J) in the frontal (F), temporal (T), parieto-occipital (PO), and cortical (C) regions in control (□) and diabetic (DM;▪) groups (means ± SE). ††Between-region comparisons for both groups ($P < 0.0001$). †$P = 0.001 \leq P \leq 0.006$. ##Between-group comparisons over all regions ($P = 0.001$). #$P = 0.005 \leq P \leq 0.006$.

Table 1

—Demographic characteristics of the control and the diabetic groups

	Control group	Diabetic group	*P*
Age (years)	60.4 ± 8.6	61.6 ± 6.6	NS
Sex (men/women)	13/12	13/13	NS
Race (white/Asian/African American)	22/1/2	21/2/3	NS
BMI (kg/m^2)	24.7 ± 2.5	27.4 ± 4.6	0.01
Diabetes duration (years)	—	12.9 ± 11.3	—
A1C (%)	5.5 ± 0.4	7.1 ± 1.0	<0.0001
Glucose	79.1 ± 16.5	133.6 ± 77.5	0.002
Systolic blood pressure (mmHg)	121.4 ± 12.2	130.5 ± 17.4	0.04
Diastolic blood pressure (mmHg)	65.9 ± 10.4	66.4 ± 9.5	NS
Hyperlipidemia (yes/no)	7/15	10/18	—
Total cholesterol (mg/dl)	226.5 ± 45.7	189.9 ± 42.7	0.007
Cholesterol-to-HDL ratio	3.72 ± 1.06	3.34 ± 1.12	NS
Triglycerides (mg/dl)	152.1 ± 73.9	234.6 ± 189.4	NS
Urinary albumin (mg/dl)	3.01 ± 4.7	2.7 ± 4.3	NS
Hypertension (yes/no)	0/25	8/18	—
Diabetic retinopathy (yes/no/missing values)	0/21/4	10/15/1	—
Hematocrit (%)	40.4 ± 2.9	38.2 ± 3.7	0.02
Whole brain (cm^3)	982.8 ± 20.6	971.5 ± 17.6	NS

Data are means ± SD unless otherwise indicated. *P* denotes between-group comparisons.